Title
Higher fusion power gain with current and pressure profile control in strongly shaped DIII-D tokamak plasmas

Journal
Physical Review Letters, 77(13)

ISSN
0031-9007

Authors
Lazarus, EA
Navratil, GA
Greenfield, CM
et al.

Publication Date
1996

DOI
10.1103/PhysRevLett.77.2714

Higher Fusion Power Gain with Current and Pressure Profile Control in Strongly Shaped DIII-D Tokamak Plasmas

E. A. Lazarus,* G. A. Navratil,† C. M. Greenfield, E. J. Strait, M. E. Austin‡ K. H. Burrell, T. A. Casper,§ D. R. Baker, J. C. DeBoo, E. J. Doyle,‖ R. Durst,¶ J. R. Ferron, C. B. Forest, P. Gohil, R. J. Groebner, W. W. Heidbrink,** R.-M. Hong, W. A. Houlberg,* A. W. Howald, C.-L. Hsieh, A. W. Hyatt, G. L. Jackson, J. Kim, L. L. Lao, C. J. Lasnier,§ A. W. Leonard, J. Lohr, R. J. La Haye, R. Maingi,†† R. L. Miller, M. Murakami,* T. H. Osborne, L. J. Perkins,§ C. C. Petty, C. L. Rettig,‖ T. L. Rhodes, B. W. Rice,§ S. A. Sabbagh,† D. P. Schissel, J. T. Scoville, R. T. Snider, G. M. Staebler, B. W. Stallard,§ R. D. Stambaugh, H. E. St. John, R. E. Stockdale, P. L. Taylor, D. M. Thomas, A. D. Turnbull, M. R. Wade,* R. Wood,§, and D. Whyte††,‡‡

General Atomics, P.O. Box 85608, San Diego, California 92186-9784

(Received 23 February 1996)

Fusion power has been increased by a factor of 3 in DIII-D by tailoring the pressure profile to avoid the kink instability in H-mode plasmas. The resulting plasmas are found to have neoclassical ion confinement. This reduction in transport losses in beam-heated plasmas with negative central shear is correlated with a dramatic reduction in density fluctuations. Improved magnetohydrodynamic stability is achieved by controlling the plasma pressure profile width. In deuterium plasmas the highest gain Q (the ratio of fusion power to input power), was 0.0015, corresponding to an equivalent Q of 0.32 in a deuterium-tritium plasma. [S0031-9007(96)01257-4]

PACS numbers: 52.55.Fa

A critical milestone in the development of controlled fusion is the production of plasma conditions with strong fusion self-heating, leading to a sustained fusion ignition condition. The ratio of fusion power to input power Q is roughly proportional to the square of the plasma pressure and generally increases with the mean strength of the confining toroidal magnetic field B_t and the size of the plasma, or major radius, R. In the DIII-D tokamak, strong shaping [1] of the plasma improves stability and allows operation at high β with good confinement, which also increases Q. Here β is the ratio of plasma pressure to magnetic field pressure.

In this paper we report a significant increase in the fusion power gain in deuterium plasmas, to $Q_{dd} = 0.0015$. This value of Q_{dd} corresponds to an equivalent Q in a deuterium-tritium plasma, $Q_{dt} = 0.32$. Record levels of plasma reactivity for DIII-D are obtained through the achievement of a neoclassical level of ion transport over most of the plasma volume. This is accomplished by control of the current profile in the target (plasma prior to application of high-power neutral beam heating) combined with improved magnetohydrodynamic (MHD) stability limits through control of the plasma pressure profile during the high-power heating phase in strongly shaped plasmas.

Recent calculations [2–4] predict that a central region with negative shear in the safety factor will enhance plasma stability. The safety factor q is the number of toroidal transits of a field line for one poloidal transit, and the shear is $(2V/q)dq/dV$ where V is the volume enclosed by the flux surface. Both fusion reactivity and plasma stability are sensitive to the form of the pressure profile. Improved core confinement with negative central shear (NCS) has been observed in both L-mode [5] and H-mode [6] DIII-D plasmas, as well as in JET [7] and TFTR [8]. H-mode plasmas are characterized by a transport barrier at the plasma edge leading to a broader pressure profile. However, NCS plasmas with an L-mode edge exhibit strongly peaked pressure profiles and invariably disrupt at beta values about a factor of 2 less than the values achieved in H mode [9]. This L-mode beta limit is consistent with ideal MHD stability limits, and broadening the pressure profile is predicted to enhance stability and result in a large increase in plasma reactivity for strongly shape plasma cross sections [10]. The key result from Ref. [10], relating β^* to the width of the pressure profile, is shown in Fig. 1. The ratio of the rms-average plasma pressure to

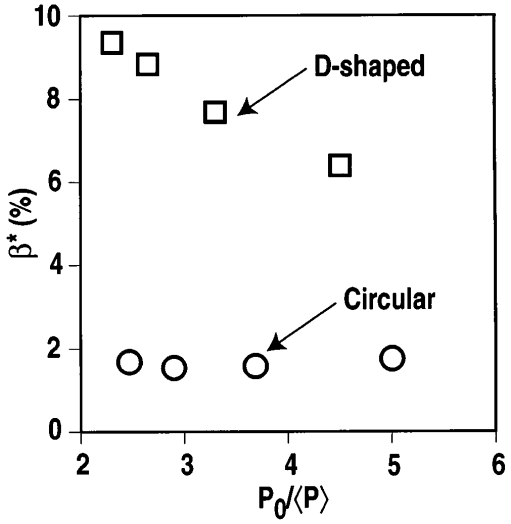

FIG. 1. The highest β^* ideally stable to the $n = 1$ (kink) mode vs the pressure peaking factor $p_0/\langle p\rangle$ for a form factor $p = p_0(1 - \rho^2)^n$. Shown are the results for a circle and a D shape with elongation 1.7 and triangularity 0.7.

 0031-9007/96/77(13)/2714(4)$10.00

the magnetic field pressure $\beta^* = 2\mu_0\langle p^2\rangle^{1/2}/B^2$ is more representative of plasma reactivity than β. Figure 1 makes the point that the effects of the pressure profile in shaped plasmas are much different than in circular plasmas where there is little sensitivity of the β^* stability limit to the pressure profile, consistent with other work [11]. The results of the computational study shown in Fig. 1 were a strong motivating force for these experiments. The experimental tool used to control the pressure profile is the timing of the L-H transition, with the transition to H mode serving to broaden the pressure profile.

This controlled transition has led to record reactivity for DIII-D plasmas, with Q_{dd} reaching values comparable to those in the larger, higher magnetic field tokamaks, JET [12], JT-60U [13], and TFTR [14]. Before discussing the details of the experiment and analysis we present a survey of the results in Fig. 2 where neutron rate S_n is plotted against heating power. The symbols distinguish the L- and H-mode plasmas. The L-mode plasmas consistently produce a lower S_n and terminate in a disruption. The pressure ratio $p_0/\langle p\rangle$ of the L-mode plasmas is in the range 4–5 while for H-mode plasmas this ratio is typically 2. The data points (shots 87937 and 87977) indicated as larger circles will be discussed in the remainder of this paper. Also shown as a triangle is shot 78136 [15], a VH-mode plasma with the highest reactivity achieved prior to the development [16] of the NCS target.

The experiment is straightforward; a target NCS plasma is created and allowed to remain in L mode until it disrupts. The discharge is repeated. About 100 ms before it would have disrupted an H-mode transition is induced, allowing the plasma to evolve.

In Fig. 3 we show the time evolution of selected quantities from 87937. The D_α emission 3(a) shows the L-H transition; also shown here are the heating power and neutron rate evolution. In 3(b) is the control signal shifting the plasma down, making the dominant X point the one in the direction of the ion ∇B drift. Also shown is the plasma response $\langle Z\rangle$ for the outer surface. Initially the plasma is shifted upwards, suppressing the H mode. The pressure profile broadening after the transition is shown in 3(c) by the decrease in $p_0/\langle p\rangle$, and the concurrent rise in β^*. The termination of the enhanced performance (2.42 s) is correlated with the onset of low toroidal mode number MHD activity. In this case, mode numbers 2 and 3 predominate, though $n = 1$ is often observed. In general this onset of MHD activity is correlated with a time when with central neutral beam deposition is reduced as a result of increased plasma density of H-mode plasmas. Prior to this MHD activity the neutral beam deposition profile is quite peaked, comparable to TFTR supershots [17].

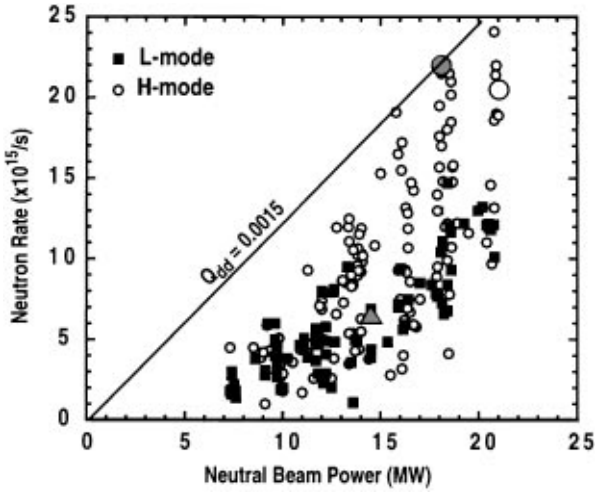

FIG. 2. Results from this experiment displayed as peak neutron rate, S_n, vs neutral beam power. The solid squares are L-mode plasmas and the open circles are H-mode. The large open circle is 87937, discussed in Fig. 3, and the large shaded circle is 87977, discussed in Figs. 4 and 5 and Table I.

We turn to 87977 (shaded large circle in Fig. 2) for which we have more complete fluctuation data to discuss the transport and fluctuation signatures observed in these H-mode plasmas. The transport analysis of 87977 is done using the TRANSP [18] analysis code. The dominant power flow is from the neutral beams to the ions with the dominant loss terms being the convection and collisonal transfer to the electron channel. We will define an effective thermal diffusivity $\chi^{\rm tot}$ as $\chi_i^{\rm tot} = Q_i^{\rm tot}/n_i\nabla T_i$. This effective ion thermal diffusivity avoids the difficulty of separating the ion heat loss into convective and conductive parts. The knowledge of the particle sources in tokamaks is incomplete making the decomposition uncertain. Additionally, there is some controversy as to the numerical coefficient of the convective term [19], and in this way we avoid prescribing a value. In the very center the neoclassical calculations is known to be in error because the ion orbits are

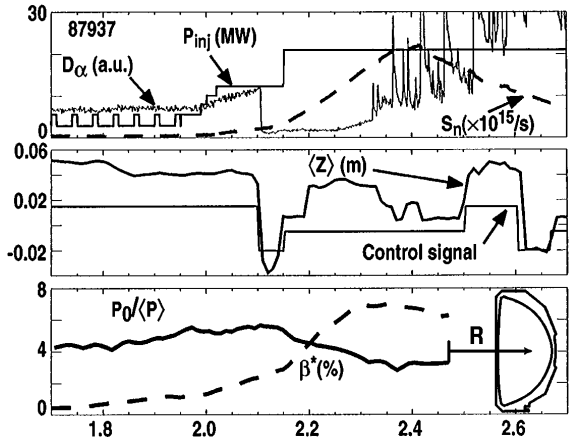

FIG. 3. The time evolution of selected quantities from 87937: (a) D_α emission from the lower divertor region showing the L-H transition at 2.12 s and the comencement of edge localized modes at 2.32 s. Also shown are the staging of the heating power and the evolution of S_n. (b) The averaged vertical plasma position used to time the L-H transition and the control signal (a.u.) for this position. (c) The evolution of the pressure profile width represented as $p_0/\langle p\rangle$, and rise in β^* resulting from the L-H transition, which correlates with rising S_n. The plasma shape and limiting surface are shown as an inset.

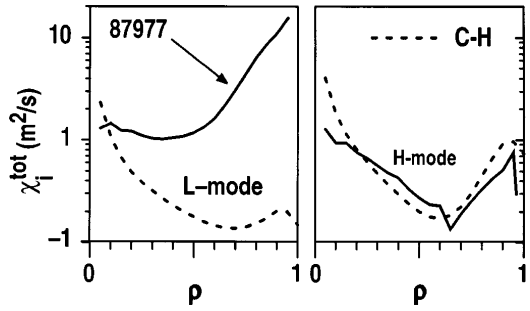

FIG. 4. Ion thermal diffusivity vs ρ, square root of the normalized toroidal flux. The solid lines are the experiment and the dashed lines are the calculated neoclassical values. (a) Representative time during the L-mode phase. (b) Diffusivity during the H-mode phase.

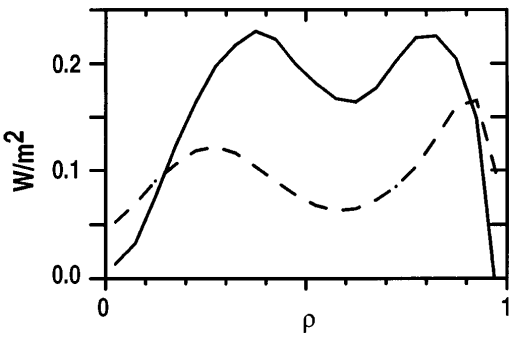

FIG. 5. Comparison of the experimental ion heat flux (solid line) for 87977 at 2.58 s with the prediction of the HS neoclassical formulation (dashed line).

too large for the ordering of the calculation to be satisfied. At the edge an error is introduced because some ion orbits will leave the confined region.

In Fig. 4(a) we compare the effective ion diffusivity χ_i^{tot} to the Chang-Hinton formula [20] for neoclassical diffusivity at a representative time during the L-mode high-power phase. The formula is derived in the limit of circular flux surfaces at finite aspect ratio with a correction accounting for an impurity concentration. The dramatic reduction in ion transport during the H-mode phase is shown in Fig. 4(b). χ_i^{tot} over the entire plasma is now comparable to the neoclassical level. The chosen time is 50 ms prior to the peak neutron rate, when β is in excess of 6%. This time is just prior to the onset of $n = 2$ MHD activity when χ_i^{tot} begins to rise again.

In Fig. 5 the ion transport is compared to a multiple ion species implementation [21] of the neoclassical force balances using the formulation of Hirshman and Sigmar (HS) [22] with the perpendicular viscosity of Shaing *et al.* [23]. This calculation is done in the equilibrium geometry. In comparing to HS we continue to avoid the decomposition into conductive and convective parts and simply compare total heat flux from the experiment to total neoclassical heat flux: $Q_{\text{ion}}^{\text{NC}} = Q_{\text{cond}}^{\text{NC}} + \frac{5}{2}\Gamma^{\text{NC}} T_i$ where $\chi^{\text{NC}} n_i \nabla T_i$ is the dominant conductive term. This is shown in Fig. 5. With this more complete treatment the experimental results are above, but still comparable to, the neoclassical result. The disagreement is less than the experimental uncertainties.

This plasma reached the highest fusion gain achieved in DIII-D (Fig. 2) and was used as the basis for projecting the reactivity of a deuterium-tritium plasma under these conditions. The evolution of 87977 is similar to 87937 shown in Fig. 3. The procedure for calculating an equivalent Q_{dt} closely follows that applied to deuterium discharges in TFTR [24]. No isotropic transport improvements were assumed. The experimental profiles (temperatures, densities, toroidal rotation) were maintained with the assumption of no transport differences between deuterium and tritium ions. The DT simulations for 87977 predict $Q_{dt} = 0.32$. The value $S_n = 2.2 \times 10^{16}$ s^{-1} was measured with a calibrated scintillator. Values of $S_n = 2.3 \times 10^{16}$ s^{-1} measured with a fission product counter and $S_n = 2.5 \times 10^{16}$ s^{-1} from calculations using the experimental temperature and density profiles provide confidence in these results. Plasma parameters are shown in Table I.

Density fluctuation spectra show good correlation with the observed behavior of the ion transport. In Fig. 6 we show the power spectra of density fluctuations observed via far-infrared scattering at a wave number of 2 cm^{-1}. The diagnostic views a large scattering volume and spatial resolution results from the Doppler shift in the plasma which has significant shear in the toroidal rotation velocity. Thus the highest frequencies correspond to the inner region ($\rho \approx 0.3$) while frequencies near zero result from light scattered from the plasma edge. A beam emission spectroscopy diagnostic observes the density fluctuations falling below a detectable level, placing the amplitude at less than 0.1% of the local density.

In conclusion, control of the pressure profile has been accomplished by selective timing of the L-H transition. The resulting increase in β^* is consistent with expectations

TABLE I. Parameters of 87977 at the time of the peak neutron rate.

$I_p = 2.25$ MA	$S_n = 2.2 \times 10^{16}$ neutrons/s
$B_t = 2.15$ T	$W = 4.2$ MJ, $\tau_E = 0.4$ s
$R_{\text{major}} = 1.67$ m	$P_{\text{NBI}} = 17.75$, $dW/dt = 7.4$ MW
$r_{\text{minor}} = 0.61$ m	$T_i(0)$, $T_e(0) = 18.1$, 7.5 keV
$\kappa = 2.15$, $\delta = 0.9$	$n_e(0)$, $n_D(0) = 10.0$, 8.5×10^{19} m^{-3}
$V_p = 22$ m^3	$\tau_E/\tau^{ITER} - 89P = 4.5$
$\beta = 6.7\%$, $\beta^* = 7.5$	$q_{95} = 4.2$, $Z_{\text{eff}} \approx 2$ (carbon)
$p(0) = 0.33$ MPa	Thermonuclear neutron fraction: 0.6

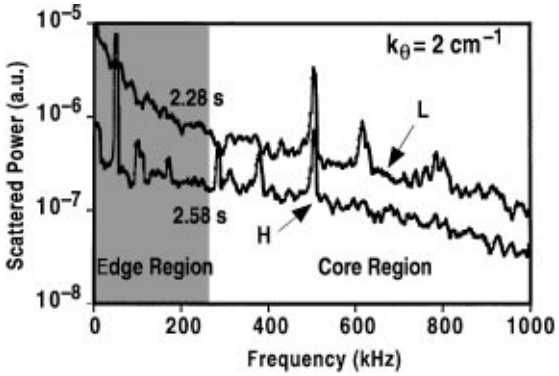

FIG. 6. Density fluctuations as observed with a far infrared scattering apparatus. The measurement observes a poloidal wave number $k_\theta = 2$ cm^{-1}.

based on ideal MHD stability calculations. The plasmas exhibit a neoclassical level of ion transport in the core during the L-mode phase, and this level extends over the entire plasma cross section after the L-H transition. While an NCS target is a necessary condition, the details of the shear do not appear to be important to the ion transport. The plasmas discussed here evolve to a weak positive shear in the region $\rho < 0.7$. Of course, the shear outside this region is strongly positive. Plasmas with increased shear reversal show similar ion transport but reduced stability in that they collapse at lower β^*. The improved energy confinement in negative magnetic shear discharges is essential in reaching high neutron rates with moderate input power. The correlation of the reduced transport with a reduction in density fluctuations suggests microturbulence as responsible for ion transport. One hypothesis which can explain the phenomenology is based on the combined effects of negative magnetic shear and stabilization of microturbulence by sheared $\mathbf{E} \times \mathbf{B}$ flow [25,26]. The negative magnetic shear allows stabilization of both macroscopic MHD modes and small scale MHD modes in the plasma core. This stabilization allows the pressure and plasma rotation in the plasma core to build up, thus increasing the radial electric field E_r. The large extent of the region of neoclassical level ion transport is consistent with theoretical modeling of $\mathbf{E} \times \mathbf{B}$ flow shear suppression of turbulence at high power [27] which can allow a transport bifurcation to develop. In these experiments in DIII-D the $\mathbf{E} \times \mathbf{B}$ flow shear is predominantly driven by toroidal rotation and not the ion pressure gradient. The improved stability and confinement has allowed DIII-D to achieve a fusion gain in deuterium plasmas of $Q_{dd} = 0.0015$, which extrapolates to $Q_{dt}^{\text{equip}} = 0.32$ in a deuterium-tritium mixture. The Q_{dd} is comparable to that achieved in larger tokamaks with higher magnetic fields.

We wish to acknowledge the excellent work of the DIII-D Operations Group without which these experiments would not be possible. This is a report of work supported by the U.S. Department of Energy under Contracts No. DE-AC03-89ER51114, No. DE-AC05-84OR21400, No. W-7405-ENG-48 and Grants No. DE-FG02-89ER53297 and No. DE-FG03-86ER53266.

*Permanent address: Oak Ridge National Laboratory, Oak Ridge, TN.
†Permanent address: Columbia University, New York, NY.
‡Permanent address: University of Maryland, College Park, MD.
§Permanent address: Lawrence Livermore National Laboratory, Livermore, CA.
‖Permanent address: University of California at Los Angeles, Los Angeles, CA.
¶Permanent address: University of Wisconsin, Madison, WI.
**Permanent address: University of California at Irvine, Irvine, CA.
††Permanent address: Oak Ridge Associated Universities, Oak Ridge, TN.
‡‡Permanent address: INRS—Energie et Materiaux, Varennes, Quebec, Canada.

[1] E. A. Lazarus *et al.,* Phys. Fluids B **3**, 2220 (1991).
[2] A. D. Turnbull *et al.,* Phys. Rev. Lett. **74**, 718 (1995).
[3] C. Kessel *et al.,* Phys. Rev. Lett. **72**, 1212 (1994).
[4] T. S. Taylor *et al.,* Plasma Phys. Controlled Fusion **36**, B229 (1994).
[5] B. W. Rice *et al.,* Nucl. Fusion (to be published).
[6] E. J. Strait *et al.,* Phys. Rev. Lett. **75**, 4421 (1995).
[7] M. Hugon *et al.,* Nucl. Fusion **32**, 33 (1992).
[8] F. M. Levinton *et al.,* Phys. Rev. Lett. **75**, 4417 (1995).
[9] B. W. Rice *et al.,* Phys. Plasmas **3**, 1983 (1996).
[10] T. S. Taylor *et al.,* Bull. Am. Phys. Soc. **40**, 1787 (1995); A. D. Turnbull *et al.,* General Atomic Report No. GA-A22324.
[11] M. Phillips, Phys. Plasmas **3**, 1673 (1996).
[12] JET Team, Nucl. Fusion **32**, 187 (1992).
[13] T. Nishitani *et al.,* Nucl. Fusion **34**, 1069 (1994).
[14] R. J. Hawryluk *et al.,* in *Plasma Physics and Controlled Nuclear Fusion Research, 1994* (International Atomic Energy Agency, Vienna, 1995), Vol. 1, p. 11.
[15] E. A. Lazarus *et al.,* in *Plasma Physics and Controlled Nucelar Fusion Research, 1994* (Ref. [14]), Vol. 1, p. 609.
[16] B. W. Rice *et al.,* Plasma Phys. Controlled Fusion **38**, 869 (1996).
[17] H. K. Park *et al.,* in *Plasma Physics and Controlled Nucelar Fusion Research, 1994* (Ref. [14]), Vol. 2, p. 3.
[18] R. J. Goldston *et al.,* J. Comput. Phys. **43**, 61 (1981).
[19] M. Zarnstorf *et al.,* in *Plasma Physics and Controlled Nucelar Fusion Research, 1994* (Ref. [14]), Vol. 1, p. 183.
[20] C. S. Chang and F. L. Hinton, Phys. Fluids **29**, 3314 (1986).
[21] W. A. Houlberg (unpublished).
[22] S. P. Hirshman and D. J. Sigmar, Nucl. Fusion **21**, 1079 (1981).
[23] K. C. Shaing *et al.,* Phys. Plasmas **3**, 965 (1996).
[24] R. V. Budny *et al.,* Nucl. Fusion **32**, 429 (1992).
[25] H. Biglari, P. H. Diamond, and P. W. Terry, Phys. Fluids B **2**, 1 (1990).
[26] K. C. Shaing, E. C. Crume, Jr., and W. A. Houlberg, Phys. Fluids B **2**, 1492 (1990).
[27] G. M. Staebler *et al.,* Phys. Plasma **1**, 99 (1994).